Embedding automated exergoeconomic analysis in constrained design optimization of high-temperature heat pumps

***Sergio Tomasinelli*[a], *Francesco Witte*[b] *and Fontina Petrakopoulou*[a]**

[a] *TU Berlin, Chair of Energy Engineering and Climate Protection, Berlin, Germany, s.tomasinelli@tu-berlin.de CA*
[b] *German Aerospace Center (DLR), Institute of Networked Energy Systems, Oldenburg, Germany*

Abstract:
Exergoeconomic analysis following the Specific Exergy Costing (SPECO) methodology provides component-level indicators that reveal whether design improvements should target thermodynamic efficiency or capital cost reduction. While multi-objective optimization of heat pumps with exergoeconomic objectives has been demonstrated in the literature, the underlying cost balance equations, fuel/product definitions, and auxiliary equations are formulated manually for each cycle topology and must be re-derived when the configuration changes. This work presents an automated framework that embeds exergoeconomic analysis as a standardized evaluation layer within a constrained optimization loop for industrial High-Temperature Heat Pumps (HTHPs). Built on the open-source ExerPy package coupled with the TESPy simulation environment, the framework automates the formulation of SPECO balance equations for arbitrary cycle topologies, enabling consistent cross-configuration comparison without manual re-derivation. The methodology is demonstrated on five HTHP configurations of increasing complexity, namely a simple cycle, an internal heat exchanger (IHX) cycle, an economizer cycle, a combined IHX with economizer cycle, and a cascade cycle, all designed for industrial steam generation at 110 °C from waste heat at 60 °C. N-butane (R600) serves as the working fluid in all configurations, while propane (R290) is employed exclusively as the working fluid of the lower temperature loop in the cascade configuration. The specific exergetic product cost c_{P} is minimized using the NSGA-II genetic algorithm. Among the investigated topologies, the IHX cycle achieves the lowest c_{P} of 140.0 €/GJ$_{\mathrm{ex}}$ with a Coefficient of Performance (COP) of 3.95 and an exergetic efficiency of 65.1%, demonstrating that cycle simplicity combined with liquid subcooling outperforms more complex multi-stage and cascade configurations for the considered application. The component-level analysis reveals that compressors account for 71–87% of the total investment cost rate across all topologies, while expansion valves contribute up to 23% of the total cost of exergy destruction plus investment through irreversibilities alone. These insights, inaccessible to aggregate performance metrics, are made systematically available for every candidate design explored during the optimization.

Keywords:
Exergy, Exergoeconomic analysis, Exergoeconomic optimization, High-temperature heat pumps.

1. Introduction

Decarbonizing industrial process heat is among the most pressing challenges of the energy transition. In Europe, the industrial sector accounted for approximately 24.6% of final energy consumption in 2023 [1], with process heat representing the dominant end-use at roughly 66% of sectoral demand [2]. A substantial fraction of this heat falls below $200\,^{\circ}\mathrm{C}$, a temperature range increasingly accessible to high-temperature heat pumps (HTHPs) [2, 3]. As a result, HTHPs have emerged as a promising low-carbon alternative to fossil-fuel-based heating across energy-intensive industries [4, 2].
The optimal working fluid depends strongly on the target supply temperature, cycle architecture, and compressor technology [4, 5, 6, 7, 8, 9, 10, 11], and the revised EU F-gas Regulation (EU) 2024/573

further reinforces the need for low-GWP or natural fluids [12]. Cascade and multi-stage configurations have been widely studied for the large temperature lifts required in industrial applications [13, 14, 15, 16, 17], alongside vapor-injection [18] and internal heat exchanger techniques [11]. Despite this breadth of work, reported COPs at supply temperatures exceeding $120\,^{\circ}\mathrm{C}$ typically range between 2 and 3 [13, 17, 19], motivating a more rigorous characterization of system performance beyond aggregate first-law metrics.

Exergy analysis quantifies the thermodynamic quality of every stream and pinpoints irreversibilities at the component level [20]. For heat pumps, the splitting of physical exergy into thermal and mechanical contributions is essential to correctly characterize components operating near the ambient temperature [21]. Exergoeconomic analysis extends this diagnostic framework by assigning monetary values to exergy streams through cost balance equations, following the SPECO approach [22], yielding component-level indicators ($\dot{C}_{\mathrm{D},k}$, f_k, r_k) that reveal whether improvement efforts should target thermodynamic efficiency or capital cost reduction [20]. The practical relevance of this hierarchy has been confirmed for HTHPs, where exergy-based criteria correctly identify improvement priorities that are often misattributed when relying solely on first-law metrics [23, 24].

The depth of exergoeconomic assessments in the HTHP literature varies considerably: several works rely on aggregate techno-economic metrics [11, 13, 19] or simplified exergy-based criteria [16, 23, 17, 24], while full component-level exergy analysis has been applied to cascade [25, 26] and transcritical [27] configurations. Component-level SPECO-based exergoeconomic frameworks have been demonstrated for two-stage cycles [28] and cascade arrangements [26, 29], including multi-objective optimization with exergoeconomic objectives [28, 29]. However, two key limitations persist: (i) the SPECO balance equations, fuel/product definitions, and auxiliary equations are formulated manually for a single, fixed cycle topology and must be re-derived when the configuration changes; and (ii) no common software framework exists to enable consistent exergoeconomic comparison across different cycle topologies. A recent perspective further calls for dedicated software to automate exergy-based analyses and seamlessly integrate them with mathematical optimization [30].

The present work addresses these limitations by proposing a methodology that embeds an automated exergoeconomic assessment as a standardized evaluation layer within a constrained optimization framework for industrial HTHP systems. Building on the ExerPy framework [31], the proposed approach (i) automates the formulation of exergy and exergoeconomic balance equations, including fuel/product definitions and auxiliary equations following the SPECO approach [22], so that no manual re-derivation is required when the cycle topology changes; and (ii) provides a topology-independent, open-source framework enabling consistent exergoeconomic comparison across different cycle configurations within the same optimization workflow. The concept is demonstrated for five representative HTHP configurations, with particular emphasis on the optimization problem formulation, the required input data, and the reproducibility across different cycle topologies.

2. Methodology

The methodology combines exergy analysis, exergoeconomic analysis, and evolutionary optimization to systematically identify cost-optimal HTHP designs. The analysis and optimization are realized using ExerPy, an open-source Python package for automated exergy and exergoeconomic analysis [31], which was extended with an optimization module that couples the thermodynamic simulation, exergy analysis, cost estimation, and exergoeconomic evaluation into a single automated loop.

2.1. Exergy and exergoeconomic analysis

The exergy and exergoeconomic analyses follow the well-established framework described in [20]. Physical exergy is split into its thermal and mechanical components [32], which is essential for defining meaningful exergetic efficiencies and cost allocations in heat pump components operating near ambient temperature. The component-level exergy balances, fuel/product definitions, and auxiliary equations follow the SPECO methodology [22], as implemented in ExerPy based on the generic for-

mulation presented in [33].
The exergoeconomic analysis assigns cost rates to all material and energy streams by formulating and solving a system of linear cost balance equations [34]. Because physical exergy is split, each material stream carries two independent cost rate variables: the thermal cost rate $\dot{C}^{\mathrm{T}}$ and the mechanical cost rate $\dot{C}^{\mathrm{M}}$, while non-material streams (power and heat) are characterized by a single cost rate $\dot{C}$. The cost balance for the k-th productive component is written as:

$$\sum_i \dot{C}_{i,k} - \sum_e \dot{C}_{e,k} + \dot{Z}_k = 0 \tag{1}$$

where $\dot{C}_{i,k}$ and $\dot{C}_{e,k}$ denote the cost rates of the inlet and outlet streams, respectively, and $\dot{Z}_k$ is the levelized cost rate of capital investment and operating and maintenance expenses associated with the k-th component. Since the number of unknown cost rates exceeds the number of cost balance equations, auxiliary equations are required to close the system. These auxiliary equations are formulated according to the F-rule and P-rule of the SPECO approach [22], which stipulate that the specific cost of exergy removed from the fuel side remains constant (F-rule) and that all exergy streams supplied on the product side receive the same specific cost (P-rule). The auxiliary equations account for the prevailing temperature levels relative to the ambient temperature, thereby ensuring physically consistent cost allocations for components that may operate across the ambient temperature level [33].
In ExerPy, the system of cost equations is constructed automatically: once the component topology and thermodynamic states are known, the framework assembles the coefficient matrix by iterating over all components and invoking their respective cost balance and auxiliary equation routines. The cost rates of all streams entering the system from external sources are specified by the user as boundary conditions. These boundary conditions, together with the cost balance and auxiliary equations, yield a square linear system that is solved for all unknown cost rates. The costs associated with dissipative components (e.g., expansion valves) and exergy loss streams are redistributed among the productive components and product streams, respectively, following the SPECO redistribution rules [22]. After the cost rates are determined, the key exergoeconomic indicators are evaluated for each component: the cost rate of exergy destruction $\dot{C}_{\mathrm{D},k} = c_{\mathrm{F},k} \cdot \dot{E}_{\mathrm{D},k}$, the relative cost difference $r_k = (c_{\mathrm{P},k} - c_{\mathrm{F},k})/c_{\mathrm{F},k}$, and the exergoeconomic factor $f_k = \dot{Z}_k/(\dot{Z}_k + \dot{C}_{\mathrm{D},k})$. These indicators quantify the contribution of each component to the overall cost formation and provide guidance for design improvements.

2.2. Exergoeconomic optimization

Conventional exergoeconomic optimization relies on manual, iterative adjustment of design parameters based on component-level indicators [20], which becomes impractical as system complexity grows. To overcome this, the present work automates the optimization by coupling the full evaluation chain into a single objective function minimized using an evolutionary algorithm. The optimization module is implemented within ExerPy and relies on pymoo [35] for single- and multi-objective optimization, with a dedicated simulation adapter for TESPy [36].
The exergoeconomic optimization is formulated as a nonlinear, bound-constrained optimization problem. The objective function is the specific exergetic product cost c_{P} [€/GJ$_{\mathrm{ex}}$], defined as the ratio of the total product cost rate to the total product exergy rate of the system:

$$c_{\mathrm{P}} = \frac{\dot{C}_{\mathrm{P,tot}}}{\dot{E}_{\mathrm{P,tot}}} = \frac{\dot{C}_{\mathrm{F,tot}} + \sum_k \dot{Z}_k}{\dot{E}_{\mathrm{P,tot}}} = \frac{c_{\mathrm{F}} \cdot \left(\dot{E}_{\mathrm{P,tot}} + \dot{E}_{\mathrm{D,tot}} + \dot{E}_{\mathrm{L,tot}}\right) + \sum_k \dot{Z}_k}{\dot{E}_{\mathrm{P,tot}}}, \tag{2}$$

whereas c_{F} and $\dot{E}_{\mathrm{P,tot}}$ are kept constant. Following the SPECO redistribution rule [22], the algorithm assigns the cost rate of any exergy loss stream $\dot{C}_{\mathrm{L,tot}}$ directly to the product streams in proportion to their exergy, so that $\dot{C}_{\mathrm{P,tot}}$ already incorporates $\dot{C}_{\mathrm{L,tot}}$. The system-level cost balance therefore

reduces to $\dot{C}_{\mathrm{P,tot}} = \dot{C}_{\mathrm{F,tot}} + \sum_k \dot{Z}_k$. This metric captures the combined effect of thermodynamic irreversibilities (through $\dot{E}_{\mathrm{D,tot}}$) and investment costs (through $\sum_k \dot{Z}_k$), inherently balancing efficiency improvements against capital expenditure.

The decision variables are continuous design parameters (e.g., heat exchanger pinch points, pressure levels, intermediate temperatures) defined with lower and upper bounds that ensure thermodynamically admissible operating points. At each candidate design point, a user-defined cost estimation function provides the component investment cost rates $\dot{Z}_k$ and boundary stream costs, from which c_{P} is computed. In the present study, these correlations are power-law functions of characteristic component size parameters, as detailed in Section 3.1..

The optimization is carried out using NSGA-II (Non-dominated Sorting Genetic Algorithm II) [37], a population-based evolutionary algorithm well suited for engineering optimization problems with nonlinear, non-convex objective landscapes. Although NSGA-II is primarily designed for multi-objective optimization, it is equally applicable to single-objective problems [35] and offers the advantage of maintaining population diversity through its crowding-distance mechanism, which reduces the risk of premature convergence to local optima [37].

3. Case study

The exergoeconomic optimization framework presented in Section 2. is applied to five HTHP topologies of increasing complexity, all designed for industrial process heat supply. The application scenario considered is the recovery of low-grade industrial waste heat, available as liquid water at $60\,^{\circ}\mathrm{C}$, to produce $1\,\mathrm{kg\,s^{-1}}$ of saturated steam at $110\,^{\circ}\mathrm{C}$ and $1.013\,\mathrm{bar}$. The waste heat source is cooled from $60\,^{\circ}\mathrm{C}$ to $50\,^{\circ}\mathrm{C}$ at atmospheric pressure. Since the source temperature lies well above the ambient temperature of $15\,^{\circ}\mathrm{C}$, the waste heat stream possesses a non-negligible exergy content and is therefore included in the system's fuel definition alongside electrical power. However, its cost is assumed to be zero, reflecting the availability of industrial waste heat at no additional charge.

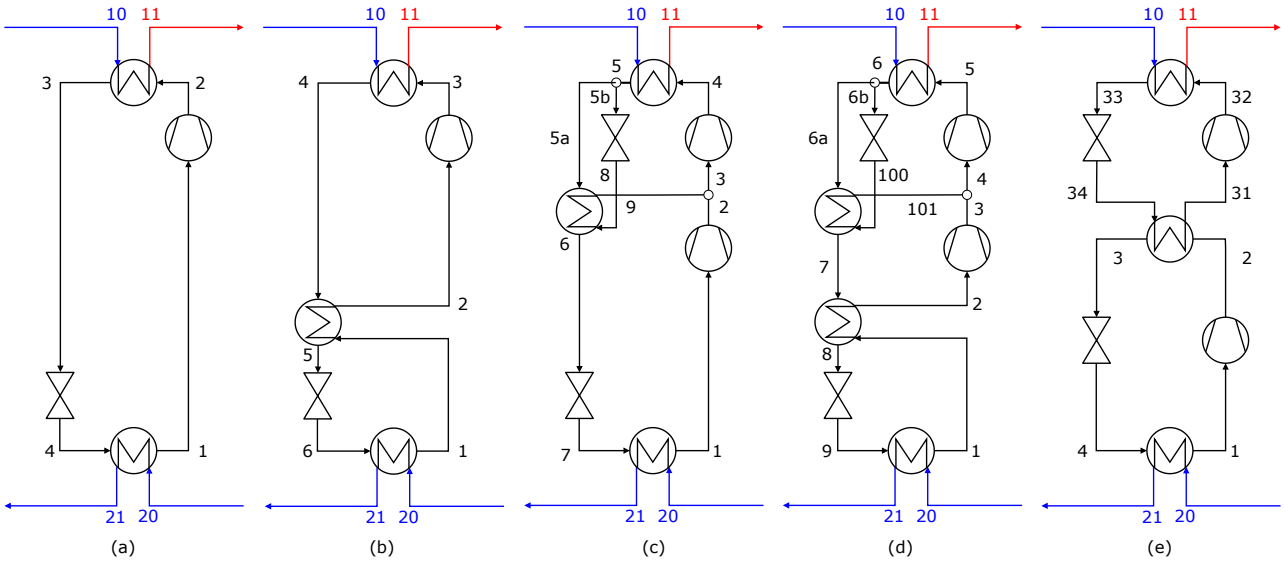

Figure 1: Schematic diagrams of the five HTHP topologies: (a) simple cycle, (b) cycle with internal heat exchanger (IHX), (c) economizer cycle (ECO), (d) combined IHX and economizer cycle, and (e) cascade cycle.

Five cycle configurations are investigated, all modeled in TESPy [36] and shown in Figure 1. All single-fluid topologies employ n-butane (R600) as the working fluid, while the cascade configuration uses propane (R290) in the low-temperature loop and n-butane in the high-temperature loop. Both fluids are natural hydrocarbons with negligible global warming potential (GWP < 5) and zero ozone depletion potential, making them fully compliant with the revised EU F-gas Regulation (EU) 2024/573 [12] and well suited for long-term industrial deployment. The simplest configuration is a single-stage subcritical cycle with n-butane (a), comprising a compressor, condenser, expansion

valve, and evaporator. The second topology extends this basic cycle with an internal heat exchanger (IHX) placed between the condenser outlet and the evaporator outlet (b), to provide liquid subcooling and suction gas superheating. The third configuration employs two-stage compression with an economizer, in which a fraction of the condensed refrigerant is expanded to an intermediate pressure level and injected between the two compressor stages (c). The fourth topology combines the IHX and the two-stage economizer arrangement in a single cycle (d). Finally, the fifth configuration is a cascade system consisting of two separate refrigerant loops: a low-temperature cycle using propane and a high-temperature cycle using n-butane (e). The two cycles are thermally coupled via a cascade heat exchanger at an intermediate temperature of $68\,^{\circ}\mathrm{C}$ in the baseline design.
All simulations are performed under steady-state conditions at the design point. The complete set of boundary conditions and thermodynamic assumptions is summarized in Table 1.

Table 1: Boundary conditions and thermodynamic assumptions.

Parameter	Value
Working fluid (single-stage & two-stage)	n-butane (R600)
Working fluid (cascade LT / HT)	propane (R290) / n-butane (R600)
Heat source inlet / outlet temperature	$60\,^{\circ}\mathrm{C}$ / $50\,^{\circ}\mathrm{C}$
Heat source fluid	Water at $1.013\,\mathrm{bar}$
Heat sink inlet / outlet temperature	$75\,^{\circ}\mathrm{C}$ / $110\,^{\circ}\mathrm{C}$ (steam)
Heat sink pressure	$1.013\,\mathrm{bar}$
Steam mass flow rate	$1\,\mathrm{kg\,s^{-1}}$
Ambient temperature T_0	$15\,^{\circ}\mathrm{C}$
Ambient pressure p_0	$1.013\,\mathrm{bar}$
Compressor isentropic efficiency η_s	0.80
Motor efficiency η_{mot}	0.985
Baseline min. temperature difference ΔT_{min}	$7\,\mathrm{K}$

The fuel of the overall system is defined as the sum of the electric power input and the exergy decrease of the waste heat source. The product exergy is linked to the exergy increase of the heated water. No exergy losses are defined, as all exergy is either converted to product or destroyed internally within the system boundary. Physical exergy is split into its thermal and mechanical components to enable the SPECO-based exergoeconomic cost allocation.

3.1. Cost estimation

The estimation of purchased equipment costs (PEC) constitutes a critical element of the economic analysis. These costs are obtained from the literature [38] and adjusted from 2013 to 2025 monetary values using the Chemical Engineering Plant Cost Index (CEPCI) [39]. The CEPCI value of 567.3 for the base year 2013 and a preliminary value of 836.5 for 2025 yield a cost index ratio of 1.4743, which accounts for inflationary effects and changes in equipment manufacturing costs over the considered time interval.
The following cost correlations refer to the base year 2013 and are expressed in euros [38]. The cost of the compressors (including the integrated electric motor for hydrocarbon refrigerants such as n-butane and propane) is calculated based on the suction volumetric flow rate ($\dot{V}$ in $\mathrm{m^3\,h^{-1}}$):

$$\mathrm{PEC_{COMP}} = 19850 \cdot \left(\frac{\dot{V}}{279.8} \right)^{0.73} \tag{3}$$

For plate heat exchangers, the cost correlation is a function of the heat transfer surface area (A in $\mathrm{m^2}$):

$$\mathrm{PEC_{HX}} = 15526 \cdot \left(\frac{A}{42} \right)^{0.8} \tag{4}$$

The heat exchanger area is calculated section-wise, assigning an overall heat transfer coefficient U to each section based on the phase of the hot-side and cold-side fluids. The values adopted from [38] are: $3696\,\mathrm{W\,m^{-2}\,K^{-1}}$ for condensing against liquid, $1483\,\mathrm{W\,m^{-2}\,K^{-1}}$ for boiling against liquid, $1494\,\mathrm{W\,m^{-2}\,K^{-1}}$ for liquid against liquid, $380\,\mathrm{W\,m^{-2}\,K^{-1}}$ for liquid against gas, and $466\,\mathrm{W\,m^{-2}\,K^{-1}}$ for gas against liquid. For phase combinations not covered in [38], the following estimates are used: $2500\,\mathrm{W\,m^{-2}\,K^{-1}}$ for condensing against boiling, $1000\,\mathrm{W\,m^{-2}\,K^{-1}}$ for condensing against gas, $750\,\mathrm{W\,m^{-2}\,K^{-1}}$ for gas against boiling, and $35\,\mathrm{W\,m^{-2}\,K^{-1}}$ for gas against gas. Expansion valves represent relatively low-cost components in the overall system configuration. For this reason, the capital expenditure of these components is neglected in the present analysis. The total PEC includes the primary components but does not account for cost items such as interconnecting piping, auxiliary components, instrumentation and control systems, electrical installations, engineering, and supervision [20]. To account for these supplementary capital requirements, the total capital investment (TCI) is estimated by applying a multiplicative factor of 6.32 to the purchase equipment costs [20]. The cost rates associated with capital investment and operation and maintenance ($\dot{Z}_k^{\mathrm{CI}}$ and $\dot{Z}_k^{\mathrm{OM}}$) are then calculated using the total revenue requirement (TRR) method [20], which levelizes the capital investment and operating and maintenance costs over the economic lifetime of the plant. The key economic assumptions are summarized in Table 2.

Table 2: Economic parameters for the exergoeconomic analysis.

Parameter	Value
Cost reference year	2013, updated to 2025 (CI ratio 1.4743)
Installation factor (TCI/PEC)	6.32 [20]
Annual full load hours	$7500\,\mathrm{h/year}$
Equipment lifetime	$20\,\mathrm{years}$
Interest rate	10%
Cost escalation rate	2%
Operating and maintenance (OM) factor	3% of TCI
Electricity cost c_{el}	80 €/GJ (0.288 €/kW h)
Heat source cost	0 €/GJ$_{\mathrm{ex}}$ (industrial waste heat)
Feedwater cost	0 €/GJ$_{\mathrm{ex}}$

3.2. Optimization setup

Each topology is optimized to minimize the specific cost of the exergy product c_{P} [€/GJ$_{\mathrm{ex}}$] using the NSGA-II genetic algorithm [37] with a population size of 50 and 40 generations, resulting in approximately 2000 thermodynamic-economic function evaluations per topology. Due to the non-convex nature of the objective landscape, particularly for topologies with more decision variables, the genetic algorithm is not guaranteed to converge to the global optimum. The baseline design uses uniform minimum temperature differences of $7\,\mathrm{K}$ for all heat exchangers and dew-point temperature differences where applicable. For each candidate design evaluated by the optimizer, the TESPy network is re-solved, followed by a complete exergy analysis and exergoeconomic evaluation including automated cost estimation via ExerPy. Table 3 lists the decision variables and their corresponding bounds for each topology.

3.3. Results and discussion

The results of the optimization are presented in Table 4, which compares the key performance indicators for both the baseline and optimized designs of all five topologies.

The IHX topology achieves the lowest specific product cost ($c_{\mathrm{P}} = 140.0$ €/GJ$_{\mathrm{ex}}$) and the lowest total $\dot{C}_{\mathrm{D}} + \dot{Z}$ (157.2 €/h), followed by the IHX+ECO cycle (155.9 €/GJ$_{\mathrm{ex}}$). The design with the internal heat exchanger reduces throttling losses by subcooling the liquid before the expansion valve and increases the COP from 3.83 to 3.95, while incurring only a moderate investment penalty. In

Table 3: Decision variables, bounds, baseline (Base) and optimized (Opt.) values for each topology.

			Simple		IHX		ECO		IHX+ECO		Cascade	
Variable	Unit	Bounds	Base	Opt.	Base	Opt.	Base	Opt.	Base	Opt.	Base	Opt.
$\Delta T_{\text{min,cond}}$	K	3–10	7.0	3.0	7.0	3.0	7.0	3.0	7.0	3.0	7.0	3.4
$\Delta T_{\text{min,evap}}$	K	3–10	7.0	3.0			7.0	3.0	7.0	3.0	7.0	3.0
$\Delta T_{\text{min,IHX}}$	K	3–10			7.0	4.0			7.0	3.7		
$\Delta T_{\text{pinch,ECO}}$	K	3–10					7.0	3.0	7.0	3.0		
p_{mid}	bar	4.5–8.6					6.7	7.8	6.7	8.6		
$\Delta T_{\text{dew,ECO}}$	K	1–15					7.0	26.2	7.0	15.0		
$\Delta T_{\text{pinch,CASC}}$	K	3–10									7.0	3.0
T_{cascade}	°C	60–80									68.0	67.7
$\Delta T_{\text{dew,LT}}$	K	1–25									7.0	10.0
$\Delta T_{\text{dew,HT}}$	K	1–25									7.0	14.7
Total variables			2		2		5		6		6	

Table 4: Baseline and optimal performance comparison for all five topologies.

		Simple		IHX		ECO		IHX+ECO		Cascade	
Indicator	Unit	Base	Opt.	Base	Opt.	Base	Opt.	Base	Opt.	Base	Opt.
c_{P}	€/GJ$_{\text{ex}}$	169.3	159.1	142.9	140.0	176.6	165.4	172.7	155.9	191.3	163.4
ε	%	58.4	60.8	63.8	65.1	62.1	64.8	62.9	68.1	55.0	67.4
COP	–	3.36	3.56	3.83	3.95	3.68	3.92	3.74	4.24	3.08	4.16
$\dot{Z}$	€/h	121.4	113.4	95.6	95.5	153.7	143.8	149.6	138.5	145.7	150.3
$\dot{C}_{\text{D}} + \dot{Z}$	€/h	207.7	190.3	161.5	157.2	225.4	206.2	218.7	190.9	247.3	204.9

fact, the total $\dot{Z}$ of the IHX cycle (95.5 €/h) is lower than that of the simple cycle (113.4 €/h), as the reduced compressor work requirement leads to a smaller and less costly compressor.

The two-stage topologies (ECO and IHX+ECO) achieve higher COPs and exergetic efficiencies. In particular, the IHX+ECO cycle reaches the highest exergetic efficiency ($\varepsilon = 68.1\%$) and COP $= 4.24$ among the single-fluid designs. However, the additional equipment leads to substantially higher investment cost rates ($\dot{Z} = 138.5$–143.8 €/h compared to 95.5 €/h for the IHX cycle), also reflected in the higher c_{P} values. The IHX+ECO topology exhibits the largest improvement upon optimization among the single-fluid topologies, reducing c_{P} by 9.8% and $\dot{C}_{\text{D}} + \dot{Z}$ from 218.7 to 190.9 €/h. This is primarily due to its six decision variables that provide greater design flexibility.

The cascade topology shows the highest $\dot{C}_{\text{D}} + \dot{Z}$ (247.3 €/h) at the baseline, of which 145.7 €/h correspond to investment costs and the remainder to the cost of the exergy destruction. Following optimization, the total $\dot{C}_{\text{D}} + \dot{Z}$ decreases to 204.9 €/h, corresponding to a c_{P} reduction of 14.6%. This improvement is primarily driven by the reduction of the heat exchanger pinch points and the increase of the compressor inlet superheat, particularly on the high-temperature stage ($\Delta T_{\text{dew,HT}}$ from $7\,\text{K}$ to $14.7\,\text{K}$). Despite the largest absolute optimization potential, the cascade configuration remains the least cost-effective topology due to the inherently higher equipment count and the thermodynamic penalty associated with the intermediate heat exchange.

Figure 2 shows the component-level contributions to the total costs of exergy destruction and investment ($\dot{C}_{\text{D}} + \dot{Z}$) for all five topologies, comparing baseline and optimized designs. The compressor group dominates the total cost in all topologies, accounting for 71–87% of the total investment cost rate $\dot{Z}$, while heat exchangers contribute only 13–29%. This cost asymmetry explains why the optimizer consistently reduces heat exchanger pinch points, as the resulting increase in heat exchanger area cost is more than offset by reduced compressor power and investment. The exergoeconomic factor f_k of the compressors ranges between 75% and 87%, confirming that their cost contribution is largely investment-dominated, whereas the condensers of the single-fluid topologies exhibit low f_k values (15–16%), indicating cost dominance by exergy destruction. The optimization consistently re-

duces the total $\dot{C}_{\mathrm{D}} + \dot{Z}$, with the most significant reductions observed for the cascade and IHX+ECO topologies. Notably, the valve components, despite their zero investment cost, contribute between 6% and 23% of the total $\dot{C}_{\mathrm{D}} + \dot{Z}$ through exergy destruction costs alone. In the simple and cascade topologies, the expansion valves represent the second-largest cost contributor (54.1 €/h and 44.4 €/h, respectively), exceeding the cost contribution of any individual heat exchanger. In contrast, the IHX and IHX+ECO topologies achieve the lowest valve costs (11.4 €/h and 13.1 €/h), as the internal heat exchanger subcools the liquid before expansion and thereby reduces throttling irreversibilities.

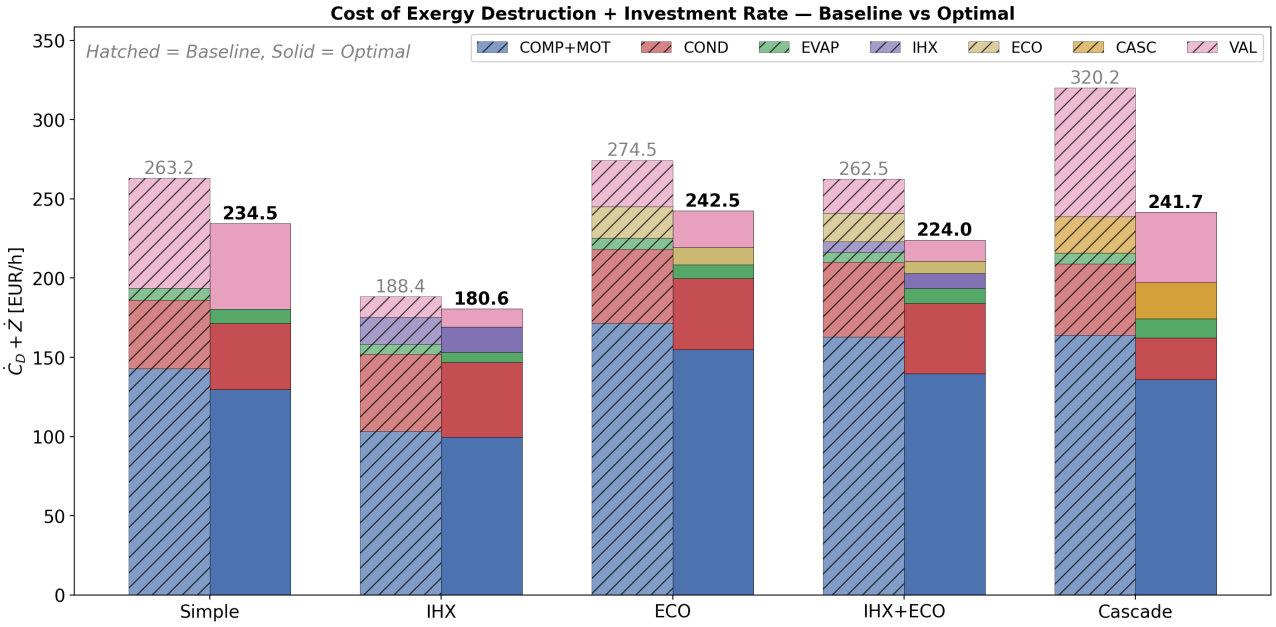

Figure 2: Component-level total cost ($\dot{C}_{\mathrm{D}} + \dot{Z}$) breakdown for all five topologies. Hatched bars represent the baseline design, solid bars the optimized design.

4. Conclusion

This work presented an automated exergoeconomic optimization framework for industrial HTHPs, implemented within the open-source ExerPy package and coupled with the TESPy simulation environment. The framework integrates thermodynamic simulation, exergy analysis, cost estimation, and exergoeconomic evaluation into a single optimization loop, thereby eliminating the need for manual iteration and ensuring methodological consistency across arbitrary system topologies.

The methodology was applied to five HTHP configurations of increasing complexity designed for industrial steam generation from waste heat. Among the investigated topologies, the IHX cycle achieved the lowest specific exergetic product cost ($c_{\mathrm{P}} = 140.0$ €/GJ$_{\mathrm{ex}}$), indicating that for the considered application, cycle simplicity combined with liquid subcooling outperforms more complex multi-stage and cascade configurations from an exergoeconomic perspective.

The use of c_{P} as the optimization objective inherently balances thermodynamic efficiency against capital investment within a single scalar metric. Beyond cost-optimal designs, the component-level diagnostic indicators ($\dot{C}_{\mathrm{D},k}$, f_k, r_k) revealed that compressors account for 71–87% of the total investment cost rate across all topologies, while expansion valves contribute significantly to $\dot{C}_{\mathrm{D}} + \dot{Z}$ through exergy destruction alone. This cost asymmetry also explains why the optimizer consistently drives heat exchanger pinch points to the lower bound of 3 K. This is due to the fact that the resulting increase in heat exchanger cost is more than compensated by reduced compressor power, investment, and exergy destruction. Such component-level insights are inaccessible to aggregate performance metrics and provide actionable guidance for targeted design improvements.

Future work should incorporate efficiency-dependent compressor cost correlations, as compressors dominate the investment structure yet their isentropic efficiency is not currently treated as a cost

driver. Additionally, integrating validated default cost models for common HTHP components would lower the entry barrier for users without access to custom cost data. Furthermore, alternative optimization algorithms and larger population sizes and generation counts should be investigated to improve convergence reliability, especially for topologies with higher-dimensional decision spaces where the current results may correspond to local rather than global optima. Extending the framework to part-load operation and coupling it with exergoenvironmental analysis would further improve the practical relevance and enable simultaneous optimization of economic and environmental performance.

Acknowledgments

Part of this work was funded by the German Federal Ministry for Economic Affairs and Climate Action (BMWK), grant number 03EI1076A (DLR), 03EI1076B (TUB), project name: "SecöndLife".

Nomenclature

Abbreviations

CASC	Cascade heat exchanger	HX	Heat exchanger
CEPCI	Chemical Engineering Plant Cost Index	IHX	Internal heat exchanger
CI	Capital investment	LT	Low-temperature (loop)
COMP	Compressor	NSGA-II	Non-dominated Sorting Genetic Algorithm II
COP	Coefficient of performance	OM	Operation and maintenance
ECO	Economizer	PEC	Purchase equipment cost
GWP	Global warming potential	SPECO	Specific exergy costing
HT	High-temperature (loop)	TCI	Total capital investment
HTHP	High-temperature heat pump	TRR	Total revenue requirement

Latin symbols

A	Surface area	$[\mathrm{m}^2]$	r	Relative cost difference	[%]
c	Specific cost	[€/GJ]	T	Temperature	$[^\circ\mathrm{C}]$
$\dot{C}$	Cost rate	[€/h]	$\dot{V}$	Volumetric flow rate	$[\mathrm{m}^3\,\mathrm{h}^{-1}]$
$\dot{E}$	Exergy rate	[kW]	$\dot{Z}$	Investment cost rate	[€/h]
f	Exergoeconomic factor	[%]	p	Pressure	[bar]

Greek symbols

Δ	Difference	[–]	ε	Exergetic efficiency	[%]
η	Efficiency	[–]			

Subscripts and superscripts

0	Ambient/reference state	mid	Intermediate
CI	Capital investment	min	Minimum
D	Destruction	mot	Motor
e	Outlet/exit stream	OM	Operation and maintenance
el	Electricity	out	Outlet
F	Fuel	P	Product
i	Inlet stream	s	Isentropic
in	Inlet	T	Thermal
k	Component index	tot	Total
M	Mechanical		

References

[1] Eurostat. *Final Energy Consumption in Industry – Detailed Statistics*. Statistics Explained, European Commission. Data extracted July 2025. Online data code: `nrg_bal_s`. 2025. URL:

https://ec.europa.eu/eurostat/statistics-explained/index.php?title=Final_energy_consumption_in_industry_-_detailed_statistics.

[2] Agne Toleikyte et al. *Heat Pumps in the European Union*. JRC Technical Report JRC139377. Luxembourg: Publications Office of the European Union, 2024. DOI: 10.2760/341494. URL: https://publications.jrc.ec.europa.eu/repository/handle/JRC139377.

[3] Elias Vieren et al. "The Potential of Vapor Compression Heat Pumps Supplying Process Heat between 100 and 200 °C in the Chemical Industry". In: *Energies* 16.18 (2023), p. 6473. DOI: 10.3390/en16186473.

[4] Cordin Arpagaus et al. "High temperature heat pumps: Market overview, state of the art, research status, refrigerants, and application potentials". In: *Energy* 152 (2018), pp. 985–1010. DOI: 10.1016/j.energy.2018.03.166.

[5] Benjamin Zühlsdorf et al. *IEA HPT Annex 58: High-Temperature Heat Pumps. Task 1 Report: Technologies*. Tech. rep. HPT-AN58-2. IEA Heat Pump Centre, 2023. URL: https://heatpumpingtechnologies.org/annex58/wp-content/uploads/sites/70/2023/09/annex-58-task-1-technologies-task-report.pdf.

[6] Andrea Zini et al. "Working fluid selection for high-temperature heat pumps: a comprehensive evaluation". In: *Energies* 17.7 (2024), p. 1556. DOI: 10.3390/en17071556.

[7] Guido Francesco Frate et al. "Analysis of suitability ranges of high temperature heat pump working fluids". In: *Applied Thermal Engineering* 150 (2019), pp. 628–640. DOI: 10.1016/j.applthermaleng.2019.01.034.

[8] Christoph Höges. "Decarbonizing Steam Generation with High Temperature HeatPumps: Refrigerant Selection and Flowsheet Evaluation". In: *14th IEA Heat Pump Conference*. 2023.

[9] Christoph Höges et al. "Choosing the optimal refrigerant in heat pumps: influence of the ecologic evaluation method". In: *Applied Thermal Engineering* 263 (2025), p. 125313. DOI: 10.1016/j.applthermaleng.2024.125313.

[10] Opeyemi Bamigbetan et al. "Theoretical analysis of suitable fluids for high temperature heat pumps up to 125 C heat delivery". In: *International journal of refrigeration* 92 (2018), pp. 185–195. DOI: 10.1016/j.ijrefrig.2018.05.017.

[11] Duy K. Hoang et al. "Thermo-economic investigation and multi objective optimization of cascade high temperature heat pump using low global warming refrigerants". In: *Applied Thermal Engineering* 279 (Nov. 2025), p. 127901. ISSN: 1359-4311. DOI: 10.1016/j.applthermaleng.2025.127901.

[12] European Parliament and Council of the European Union. *Regulation (EU) 2024/573 of the European Parliament and of the Council of 7 February 2024 on fluorinated greenhouse gases, amending Directive 2019/1937/EU and repealing Regulation (EU) No 517/2014*. Regulation L 2024/573. Entered into force 11 March 2024. Official Journal of the European Union, Feb. 2024. URL: https://eur-lex.europa.eu/legal-content/EN/TXT/PDF/?uri=OJ:L_202400573.

[13] Zhenneng Lu et al. "Thermodynamic and Economic Analysis of a High Temperature Cascade Heat Pump System for Steam Generation". In: *Processes* 10.9 (2022), p. 1862. DOI: 10.3390/pr10091862.

[14] Xiaoqiong Li et al. "Performance analysis of high-temperature water source cascade heat pump using BY3B/BY6 as refrigerants". In: *Applied Thermal Engineering* 159 (Aug. 2019), p. 113895. ISSN: 1359-4311. DOI: 10.1016/j.applthermaleng.2019.113895.

[15] Liangfeng Xu et al. "An experimental energy performance investigation and economic analysis on a cascade heat pump for high-temperature water in cold region". In: *Renewable Energy* 152 (June 2020), pp. 674–683. ISSN: 0960-1481. DOI: 10.1016/j.renene.2020.01.104.

[16] Shengming Dong et al. “Investigation of cascade high temperature heat pump optimal design theory based on experiment supporting multi-objective optimization”. In: *Energy Conversion and Management* 267 (Sept. 2022), p. 115873. ISSN: 0196-8904. DOI: 10.1016/j.enconman.2022.115873.

[17] Zhangxiang Wu et al. “Performance analysis and multi-objective optimization of the high-temperature cascade heat pump system”. In: *Energy* 223 (2021), p. 120097. DOI: 10.1016/j.energy.2021.120097.

[18] Jiaheng Chen et al. “Energy, exergy, economic and environmental analyses and optimization of a novel vapor injection autocascade heat pump for high-temperature water heating”. In: *Energy Conversion and Management* 267 (2022), p. 115909. DOI: 10.1016/j.enconman.2022.115909.

[19] Xudong Ma et al. “Enhanced thermal output from air-source cascade heat pumps configuration for steam generation”. In: *Case Studies in Thermal Engineering* 75 (Nov. 2025), p. 107112. ISSN: 2214-157X. DOI: 10.1016/j.csite.2025.107112.

[20] Adrian Bejan et al. *Thermal design and optimization*. John Wiley & Sons, 1995.

[21] S. Kelly et al. “Advanced exergetic analysis: Approaches for splitting the exergy destruction into endogenous and exogenous parts”. en. In: *Energy* 34.3 (Mar. 2009), pp. 384–391. ISSN: 03605442. DOI: 10.1016/j.energy.2008.12.007. URL: https://linkinghub.elsevier.com/retrieve/pii/S036054420800323X (visited on 05/21/2025).

[22] Andrea Lazzaretto et al. “SPECO: A systematic and general methodology for calculating efficiencies and costs in thermal systems”. In: *Energy* 31.8-9 (2006), pp. 1257–1289. DOI: 10.1016/j.energy.2005.03.011.

[23] Mengying Wang et al. “Exergoeconomic performance comparison, selection and integration of industrial heat pumps for low grade waste heat recovery”. In: *Energy Conversion and Management* 207 (2020), p. 112532. DOI: 10.1016/j.enconman.2020.112532.

[24] Brendon de Raad et al. “Identifying techno-economic improvements for a steam-generating heat pump with exergy-based cost minimization”. In: *Applied Thermal Engineering* 267 (2025), p. 125632. DOI: 10.1016/j.applthermaleng.2025.125632.

[25] Xiaowei Hu et al. “Comparison study of conventional and advanced exergy analysis on cascade high temperature heat pump system based on experiment”. In: *Case Studies in Thermal Engineering* 40 (Dec. 2022), p. 102552. ISSN: 2214-157X. DOI: 10.1016/j.csite.2022.102552.

[26] Xiaowei Hu et al. “Advanced Exergy and Exergoeconomic Analysis of Cascade High-Temperature Heat Pump System for Recovery of Low-Temperature Waste Heat”. In: *Energies* 17.5 (2024), p. 1027. DOI: 10.3390/en17051027.

[27] Yuxiang Zhang et al. “Experimental study on energy, exergy, and exergoeconomic analyses of a novel compression/ejector transcritical CO2 heat pump system with dual heat sources”. In: *Energy Conversion and Management* 271 (Nov. 2022), p. 116343. ISSN: 0196-8904. DOI: 10.1016/j.enconman.2022.116343.

[28] Ammar M. Bahman et al. “Multi-objective optimization of a cold-climate two-stage economized heat pump for residential heating applications”. In: *Journal of Building Engineering* 46 (2022), p. 103799. DOI: 10.1016/j.jobe.2021.103799.

[29] Alireza Bakhtiari et al. “Multi-objective economic and exergoeconomic optimization of a cascade-configured solar-geothermal heat pump for high-temperature applications”. In: *Results in Engineering* 29 (Mar. 2026), p. 108752. ISSN: 2590-1230. DOI: 10.1016/j.rineng.2025.108752.

[30] George Tsatsaronis. “The future of exergy-based methods”. In: *Energy* 302 (2024), p. 131881. DOI: 10.1016/j.energy.2024.131881.

[31] Sergio Tomasinelli et al. “ExerPy: An open-source framework for automated exergy analysis”. In: *Journal of Open Source Software* (in preparation).

[32] Tatiana Morosuk et al. “Splitting physical exergy: Theory and application”. In: *Energy* 167 (2019), pp. 698–707. DOI: 10.1016/j.energy.2018.10.090.

[33] Francesco Witte et al. “Generic and Open-Source Exergy Analysis—Extending the Simulation Framework TESPy”. In: *Energies* 15.11 (2022), p. 4087. DOI: 10.3390/en15114087.

[34] A Valero et al. “A general theory of exergy saving. I. On the exergetic cost”. In: *Computer-aided engineering and energy systems: second law analysis and modelling* 3 (1986), pp. 1–8.

[35] Julian Blank et al. “pymoo: Multi-Objective Optimization in Python”. In: *IEEE Access* 8 (2020), pp. 89497–89509. DOI: 10.1109/ACCESS.2020.2990567.

[36] Francesco Witte et al. “TESPy: Thermal Engineering Systems in Python”. In: *Journal of Open Source Software* 5.49 (2020), p. 2178. DOI: 10.21105/joss.02178.

[37] Kalyanmoy Deb et al. “A Fast and Elitist Multiobjective Genetic Algorithm: NSGA-II”. In: *IEEE Transactions on Evolutionary Computation* 6.2 (2002), pp. 182–197. DOI: 10.1109/4235.996017.

[38] Torben Ommen et al. “Technical and economic working domains of industrial heat pumps: Part 1–Single stage vapour compression heat pumps”. In: *International Journal of Refrigeration* 55 (2015), pp. 168–182. DOI: 10.1016/j.ijrefrig.2015.02.012.

[39] Chemical Engineering. *Chemical Engineering Plant Cost Index (CEPCI)*. https://www.chemengonline.com/plant-cost-index/. Retrieved March 26, 2026. Dec. 2025.